DIAMOND, R. (1969). *Acta Cryst.* A**25**, 43–55.
FREEMAN, H. C., GUSS, J. M., NOCKOLDS, C. E., PAGE, R. & WEBSTER, A. (1970). *Acta Cryst.* A**26**, 149–152.
GRANT, D. F. (1973). *Acta Cryst.* A**29**, 217.
HANSON, J. C., WATENPAUGH, K. D., SIEKER, L. & JENSEN, L. H. (1979). *Acta Cryst.* A**35**, 616–621.
LEHMANN, M. S. & LARSEN, F. K. (1974). *Acta Cryst.* A**30**, 580–584.
NORRESTAM, R. (1972). *Acta Chem. Scand.* **26**, 3226–3234.
SLAUGHTER, M. (1969). *Z. Kristallogr.* **129**, 307–318.
TICKLE, I. J. (1975). *Acta Cryst.* B**31**, 329–331.
WAL, H. R. VAN DER, DE BOER, J. L. & VOS, A. (1979). *Acta Cryst.* A**35**, 685–688.
WATSON, H. C., SHOTTON, D. M., COX, J. M. & MUIRHEAD, H. (1970). *Nature (London)*, **225**, 806–811.
WERNER, S. A. (1972). *Acta Cryst.* A**28**, 143–151.

Acta Cryst. (1981). A**37**, 28–35

Electron Microscopy of Oxyborates. I. Defect Structures in the Minerals Pinakiolite, Ludwigite, Orthopinakiolite and Takéuchiite

BY JAN-OLOV BOVIN,* M. O'KEEFFE AND M. A. O'KEEFE†

Chemistry Department and Center for Solid State Science, Arizona State University, Tempe, Arizona 85281, *USA*

(*Received* 19 *October* 1979; *accepted* 13 *June* 1980)

Abstract

Crystals of the minerals pinakiolite $(Mg,Mn)_{1.77}(Mn,Al,Fe)_{1.11}BO_5$, ludwigite $(Mg,Fe)_2Fe^{3+}BO_5$, orthopinakiolite $(Mg,Mn)_{1.85}(Mn^{3+},Fe^{3+})BO_5$ and takéuchiite $(Mg,Mn)_{1.97}Mn^{3+}_{0.78}Fe^{3+}_{0.19}BO_5$ have been investigated by high-resolution transmission electron microscopy. Calculated and experimental images have been matched to ensure a proper interpretation. All the minerals except ludwigite show structural defects which give insight into structural relations in the pinakiolite family. It is shown that they can be described as chemical twinnings of pinakiolite. The most common defects can be described as missing twin operations.

Introduction

This investigation of oxyborates includes the minerals pinakiolite, ludwigite, orthopinakiolite and takéuchiite all with the general formula M_3BO_5, where M stands for different combinations of mainly the ions Mg^{2+}, Mn^{2+}, Fe^{2+}, Mn^{3+} and Fe^{3+}. The crystal structures of pinakiolite, ludwigite and orthopinakiolite have been determined and refined by several groups in the past. Thus the structure of pinakiolite was determined by Takéuchi, Watanabé & Ito (1950) and refined by Moore & Araki (1974). The ludwigite structure was first determined by Takéuchi *et al.* (1950) and several synthetic ferromagnetic compounds with the same structure were reported by Bertaut (1950). The structure of orthopinakiolite was solved by Takéuchi, Haga, Kato & Miura (1978). The present investigation of oxyborates also revealed a new member of the pinakiolite family: takéuchiite (Bovine & O'Keeffe, 1980). Its structure has not yet been determined by X-ray methods but has been deduced from a suggested model (Takéuchi, 1978) by comparing high-resolution

Table 1. *Chemical formula for* M_3BO_5 *minerals related to pinakiolite*

Mineral & reference	Structural formula
Pinakiolite Moore & Araki (1974)	$Mg_{1.68}Mn^{2+}_{0.09}Mn^{3+}(Al^{3+},Fe^{3+},Mn^{4+})_{0.11}BO_5$
Hulsite Konnert *et al.* (1976)	$Mg_{0.64}Fe^{2+}_{1.46}Fe^{3+}_{0.67}Sn^{4+}_{0.20}BO_5$
Ludwigite Takéuchi *et al.* (1950)	$(Mg,Fe^{2+})_2Fe^{3+}BO_5$
Vonsenite Takéuchi (1956)	$Mg_{0.75}Fe^{2+}_{1.25}Fe^{3+}BO_5$
Orthopinakiolite Takéuchi *et al.* (1978)	$Mg_{1.42}Mn^{2+}_{0.43}Mn^{3+}_{0.88}Fe^{3+}_{0.22}BO_5$
Takéuchiite Bovin & O'Keeffe (1980, 1981)	$Mg_{1.59}Mn^{2+}_{0.42}Mn^{3+}_{0.78}Fe^{3+}_{0.19}Ti^{4+}_{0.01}BO_5$

* Permanent address: Inorganic Chemistry 2, Chemical Centre, PO Box 740, S-220 07, Lund 7, Sweden.
† Present address: University of Cambridge, Department of Physics, Old Cavendish Laboratory, Cambridge CB2 3RQ, England.

0567-7394/81/010028-12$01.00

Table 2. *Crystal data for pinakiolite-related minerals*

Mineral	a (Å)	b (Å)	c (Å)	β (°)	Space group
Pinakiolite	21·79	5·977	5·341	95·83	$C2/m$
Hulsite	10·695	3·102	5·431	94·21	$P2/m$
Ludwigite	9·14	12·45	3·05		$Pbam$
Vonsenite	9·73	12·35	3·05		$Pbam$
Orthopinakiolite	18·375	12·591	6·068		$Pnnm$
Takéuchiite	27·50	12·614	6·046		$Pnnm$

electron microscopy images with calculated ones (Bovin, O'Keeffe & O'Keefe, 1981). Structural relations between the above mentioned minerals have been discussed from several points of view in several papers (Takéuchi, 1978; Takéuchi *et al.*, 1950 and Moore & Araki, 1974). The synthetic compound $NaMg_3Mn_3B_2O_{11}$ is reported (Nielsen, Søtofte, Thorup & Norrestam, 1978) to have a structure derived from that of ludwigite (the unit-cell parameters are similar to those of ludwigite).

The aim of the present investigation with high-resolution electron microscopy was to reveal the true structure, including the different types of defects, of crystals from the members of the pinakiolite family. This was expected to give insight into structural relationships and crystal growth mechanisms. In order to obtain a more complete background for such efforts a similar study of synthetic crystals of members of this structural family was carried out and the results are given in the following paper (Bovin & O'Keeffe, 1981).

Chemical formulae for M_3BO_5 minerals related to pinakiolite are given in Table 1 and the crystal data for the same minerals are given in Table 2.

Experimental

Specimens of the different minerals used in this investigation were kindly made available to us from the Smithsonian Institution, Washington, DC, USA and from the Swedish Museum of Natural History (Naturhistoriska Riksmuseet) in Stockholm, Sweden. The specimens were pinakiolite (Smithsonian no. B12313 and Naturhistoriska Riksmuseet no. R31527), ludwigite (Smithsonian no. 96984), orthopinakiolite (Naturhistoriska Riksmuseet no. R332376) and takéuchiite (Smithsonian no. 138548, labeled orthopinakiolite).

Single crystals of the mineral were ground in acetone in an agate mortar and then deposited on a holey carbon film for image recording in an electron microscope, JEOL 100 B, operated at 100 kV and equipped with a standard point filament. Correction of objective-lens astigmatism was carried out on the carbon support film by minimizing the contrast.

It was difficult to find crystal flakes with edges thin enough to obtain structure images recorded with the beam parallel to the shortest axis (**c** in all structures except pinakiolite for which it is **b**). Most images presented here come from rather thick crystals and it has been necessary to calculate images from the structural parameters of the different minerals using the multislice method (Goodman & Moodie, 1974; Cowley & Moodie, 1957), with a program developed (by MAO'K) from those of Fejes (1973), O'Keefe (1975) and Skarnulus (1976), for a proper identification of the images obtained from the different minerals. Through-focus series of images for different crystal thicknesses were calculated. Parameters used in the calculations were: incident beam convergence = 1·2 mrad, spherical aberration constant $c_s = 2{\cdot}2$ mm, focus spread due to chromatic aberration = 150 Å and aperture radius = 0·45 $Å^{-1}$. The beam convergence and aperture radius were measured from a test diffraction pattern (O'Keefe & Sanders, 1975). The values of C_s and focus spread have been estimated for our microscope by matching many computed and experimental micrographs (O'Keefe, Buseck & Iijima, 1978).

Structures and structure images

All the structures of the pinakiolite family have some common features. The length of one axis of the unit cell is a multiple of the edge length of a metal–oxygen octahedron: approximately 3 Å (*cf.* Table 2). An idealized projection of the structures along this direction show the anions situated on the vertices of a triangular net (3^6). The cations occur in this projection either at triangle centers (boron) or at the midpoint of a rhombus formed by two triangles sharing an edge (this corresponds to octahedral coordination of the heavy cations). The short projection distance and the large boron–boron distances (>5 Å) make this family of structures ideal for a transmission electron microscopy study.

The parent structure of pinakiolite is drawn in a projection along **b** in Fig. 1(*a*). In this idealized drawing the cation-centered octahedra are illustrated as red or yellow rhombi. The boron atoms are shown as large open circles. The structure contains two types of slabs of octahedra ('walls'); one consists of edge-sharing octahedra generating a flat wall [the *F* wall according to Takéuchi (1978)] marked yellow in Fig. 1(*a*), the

other wall, shown in red, consists also of corner- and edge-sharing octahedra but now arranged to give a zig-zag pattern. The two kinds of wall are alternately connected to each other by corner-sharing as shown in Fig. 1(*a*). For a detailed description of the occupancy of the octahedra see Moore & Araki (1974).

When a thin crystal was oriented so that the electron beam was parallel to **b**, showing an electron diffraction pattern like the one in Fig. 2, the structure image usually looked like the ones in Fig. 3. The two images of the same crystal edge are recorded with a difference of −750 Å in focus. The thickness of the crystal is estimated to be $30 \times (b/2) \simeq 90$ Å judged from the good agreement between calculated images of the defocus −900 Å (left) and −1600 Å and experimental ones as shown in Fig. 3. The image matching shows that in images of thin crystals recorded at an underfocus of approximately −1000 Å the white spots correspond to the boron atom positions and the zig-zag walls show up as black broad lines. But usually the thickness of the crystal increases rapidly from the edge with corresponding changes in the experimental image. This is illustrated in Fig. 4 to serve as a guide for interpretation of images (shown later) of pinakiolite (*cf.* Bovin & O'Keeffe, 1981).

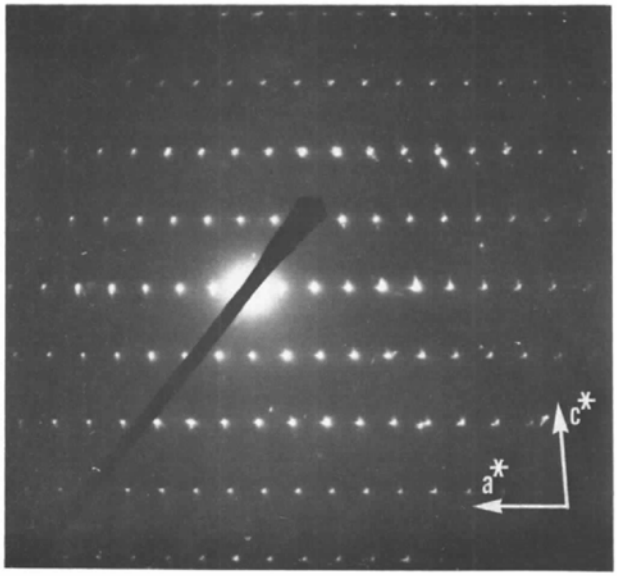

Fig. 2. Electron diffraction pattern of a pinakiolite crystal recorded with the electron beam parallel to **b**.

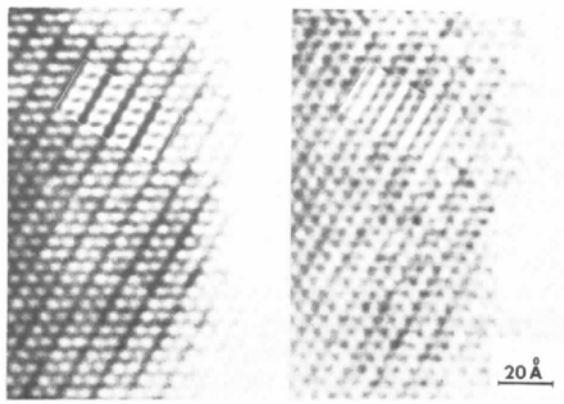

Fig. 3. Two electron micrographs of the same pinakiolite crystal edge recorded with a difference of 750 Å in underfocus. Images calculated for a crystal thickness of 90 Å and underfocus of −900 Å (on the left) and −1600 Å are inserted. The origin of the unit cell is in the upper left corner of the calculated images.

Structural defects and structural relationships

Crystals of pinakiolite often showed structural defects of the kind imaged in Fig. 4. These give important clues to the relationships between the structures of pinakiolite and other members of the family. In Fig. 5 a part of the image of Fig. 4 is enlarged and a (010) projection of the structure inserted. The defect marked 1 in the image can be interpreted as generated by the slip mechanism shown in Fig. 6. The slip vector is parallel to [201] in the pinakiolite unit cell given by Moore & Araki (1974) and has a length of two times the edge of the rhombus in Fig. 6(*a*). However the simple slip creates an unrealistic face-sharing of octahedra in the slip plane. This implies that the mechanism also must include a rearrangement of the cations in the green octahedra [*cf.* Fig. 6(*b*)]. If the cations change positions to the green octahedra of Fig. 6(*c*) the structure of the defect becomes more plausible. This model corresponds well with the image of the crystal in Fig. 5. The two other defects in the image, marked 2 and 3 in Fig. 5, can be explained as generated by pairs of slip operations. The resulting structures are shown as in

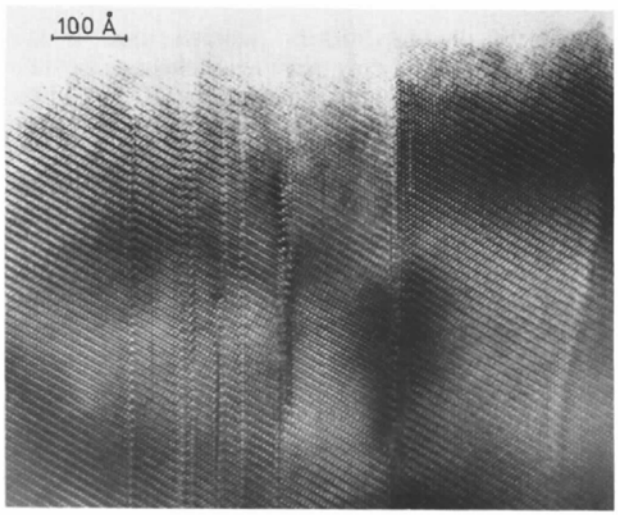

Fig. 4. Electron micrograph of a pinakiolite crystal oriented with **b** parallel to the electron beam. The crystal shows several structural defects, but the image will also serve as a guide for interpretation of pinakiolite images shown later.

Fig. 7 in which the slip planes are marked with arrows. It is a remarkable fact that the green and blue octahedra of the defects include the unit cells of ludwigite (1), orthopinakiolite (2) and takéuchiite (3). Thus the structure of ludwigite [*cf.* Fig. 1(*b*)] can be generated by a periodic repeat of the slip mechanism shown in Fig. 6. In the (001) projection of the ludwigite structure shown in Fig. 1(*b*) the slip planes are marked with broken arrows.

There is another simple relation between the structures of pinakiolite and ludwigite illustrated in Fig. 1. Two almost identical units can be found as outlined by dashed lines in the drawings. The only difference between the two is in the two octahedra marked green. The same two octahedra are also involved in the slip mechanism of Fig. 6. The structures of pinakiolite and ludwigite can obviously intergrow at a structure boundary comprised of such units. This has been found to be the case in synthetic crystals (Bovin & O'Keeffe, 1981).

The distance between two slip planes in the structure of ludwigite can be expressed in terms of the number of octahedral layers, here four [*cf.* Fig. 1(*b*)]. If the same slip mechanism is used on the structure of pinakiolite but the repeat distance is increased to six octahedral layers, then the structure shown in Fig. 8 is generated. This hypothetical relative to ludwigite is not known, but the unit cell should be close to $a = 13{\cdot}0$, $b = 3{\cdot}0$, $c = 12{\cdot}5$ Å and $\beta = 102°$. It is important to point out that even if the ludwigite structure can be generated by the slip mechanism it is not possible to generate the structure of orthopinakiolite and takéuchiite by the same mechanism.

To relate the structures of orthopinakiolite and takéuchiite to pinakiolite it is necessary to apply a chemical twinning mechanism (Andersson & Hyde, 1974). The mechanism is illustrated in Fig. 9. The twin plane, marked with arrows, is parallel to the slip planes used before (*cf.* Fig. 6). The twin axis (rotation axis) is perpendicular to this plane and runs through the center of a boron triangle. If the twin operation is carried out as in Fig. 9 the two parts of the structure join together without any change of cation sites as in the slip mechanism. Such a twin structure has not yet been found in crystals of the mineral pinakiolite, but it has been found frequently in synthetic crystals (*cf.* Fig. 6 and Fig. 9 of Bovin & O'Keeffe, 1981). The twin operation in the pinakiolite structure does not generate a new polyhedron type in the twin plane as is often the case in chemical twinnings (*cf.* Andersson & Hyde, 1974), but it is possible that the mechanism allows slightly different octahedra in the real structure. If the twin operation is carried out periodically, with a repeat of two octahedral layers, the ludwigite structure is obtained. The structure of ludwigite can thus be generated by both the mechanisms as illustrated in Fig. 1(*b*) where the twin planes are marked with arrowheads.

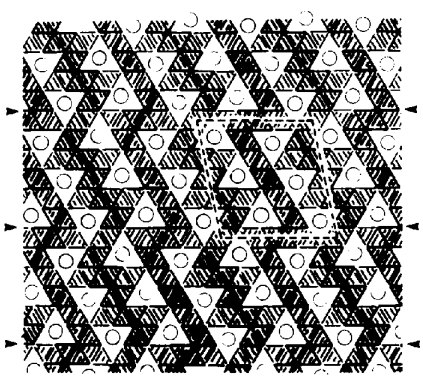

Fig. 8. Drawing of a hypothetical structure generated from pinakiolite by means of the slip mechanism (*cf.* Fig. 6). The distance between the slip planes is six octahedral layers broad [compared to four for ludwigite, *cf.* Fig. 1(*b*)].

The next possible twin repeat consists of four octahedral layers and this generates the structure of orthopinakiolite as shown in Fig. 10. A repeat of six octahedral layers gives the structure (*cf.* Bovin, O'Keeffe & O'Keefe, 1981) of the next member, takéuchiite, as illustrated in Fig. 11.

For convenience a short symbolism for structures shown so far is introduced. The symbol consists of numbers equal to the number of octahedral layers between planes symbolized by letters (*s* for slip and *t* for twin). Thus the structure of ludwigite is symbolized $2t2t\ldots$, orthopinakiolite is $4t4t\ldots$, and takéuchiite is $6t6t\ldots$. Note that ludwigite can also be written $4s4s\ldots$. An obvious possibility for defects in crystals is a mixture of mechanism and layer width, and new structures are easily devised such as $4t4s4t4s\ldots$ (unit cell $a \simeq 27{\cdot}5$ Å) or $4t4t4s4t\ldots$.

The crystal structures of ludwigite, orthopinakiolite and takéuchiite all have b in common (*cf.* Table 2) while a varies according to the number of octahedral layers between the twin planes. The distance between two oxygen layers along **a** is very similar for the three structures (2·29, 2·30 and 2·29 Å, respectively) and the electron diffraction patterns are of course very similar as shown in Fig. 12. a is given by $2n \times 4{\cdot}6$ Å where $n = 1,2,3\ldots$.

The defects in pinakiolite crystals of the kind shown in Fig. 5 will certainly affect X-ray diffraction structure determinations. It is worth pointing out that in the published X-ray investigation (Moore & Araki, 1974) two positions Mg(1) and Mg(2) were refined as partly unoccupied (~20%). Both positions also show relatively high temperature factors. Notice that Mg(1) corresponds to one of the octahedra marked green in Fig. 1(*a*), the one involved in the slip mechanism. Partial occupancy in a structure like this is rather unlikely, and one explanation of the difficulties in refinement presented by the Mg(1) and Mg(2) positions is that it is due to the presence of defects in the crystals

used. In fact, replacing the 'vacancies' with Mn^{2+} gives a charge-balanced formula, $Mg_{1\cdot8}Mn^{2+}_{0\cdot19}Mn^{3+}Fe_{0\cdot01}BO_5$ (32·5% Mn and 21·8% Mg) more in agreement with the ion-probe analysis (*cf.* Moore & Araki, 1974) than the formula assumed by Moore & Araki (1974).

Ludwigite as a mineral never showed any structural defects, although crystals from several localities were investigated. Synthetic ludwigites on the other hand showed many kinds of defects (*cf.* Bovin & O'Keeffe, 1981). The electron diffraction patterns [*cf.* Fig. 12(*a*)] and images (*cf.* Fig. 13) of ludwigite always showed lower symmetry than suggested by Takéuchi *et al.* (1950), possibly due to dynamical effects. A typical electron micrograph of a ludwigite crystal is shown in Fig. 13. Notice how it is possible to interpret the far lower left part with its thin part of the crystal as a structural image closely related to the structure drawing in Fig. 1(*b*) with the boron triangles as white spots in the image. But in thicker regions of the crystal the symmetry of the image changes and the question arises as to whether this is due to a slight mistilt or a true lower symmetry. Neither images calculated with changed cation arrangements of lower symmetry nor images calculated with mistilt of the electron beam included matched experimental images well. The image in Fig. 13 is shown to serve as a guide, and will later be used for the interpretation of images of synthetic ludwigites (*cf.* Bovin & O'Keeffe, 1981).

In contrast to crystals of ludwigite, orthopinakiolite crystals are always rich in defects. Fig. 14 illustrates how the image of an orthopinakiolite crystal changes with crystal thickness. Inserted in the upper right corner is an image of a thin crystal with the matching calculated image (underfocus −600 Å, crystal thickness 90 Å). The image is closely related to the structure drawing in Fig. 10 if the zig-zag octahedral

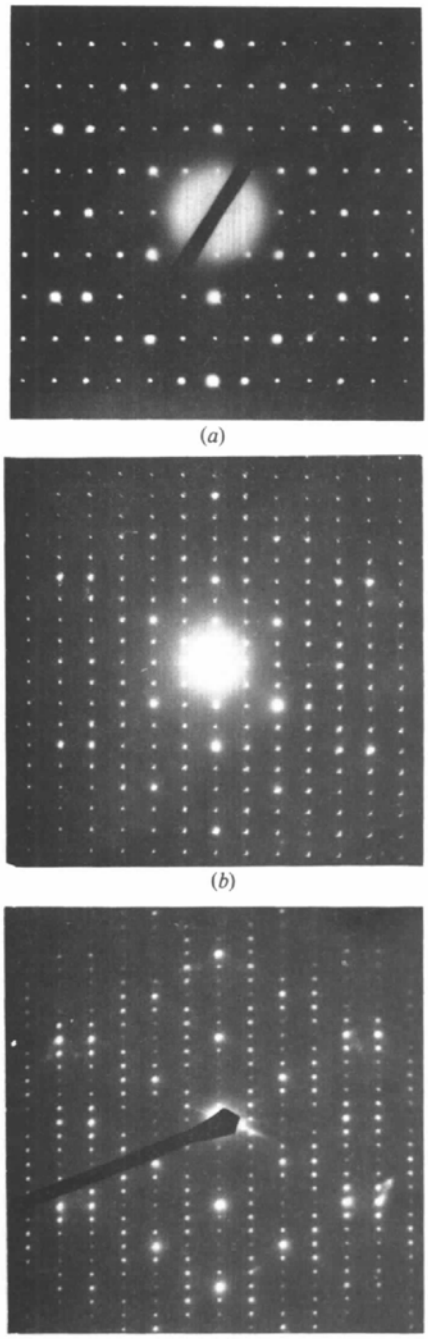

(*a*)

(*b*)

(*c*)

Fig. 12. Electron diffraction pattern for (*a*) ludwigite, (*b*) orthopinakiolite and (*c*) takéuchiite recorded with the electron beam parallel to **c**. The patterns are oriented so that **b*** is horizontal and **a*** is vertical in each case.

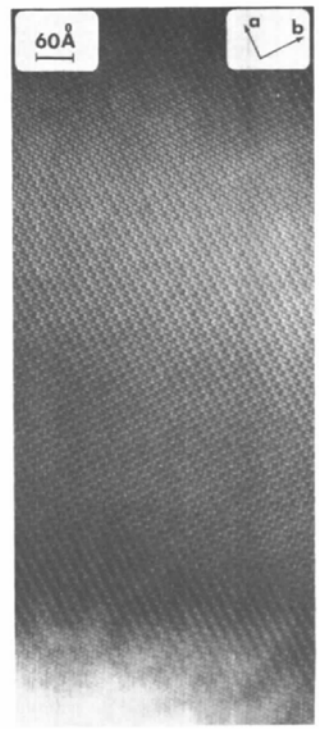

Fig. 13. Electron micrograph of a ludwigite crystal recorded with the electron beam parallel to **c**.

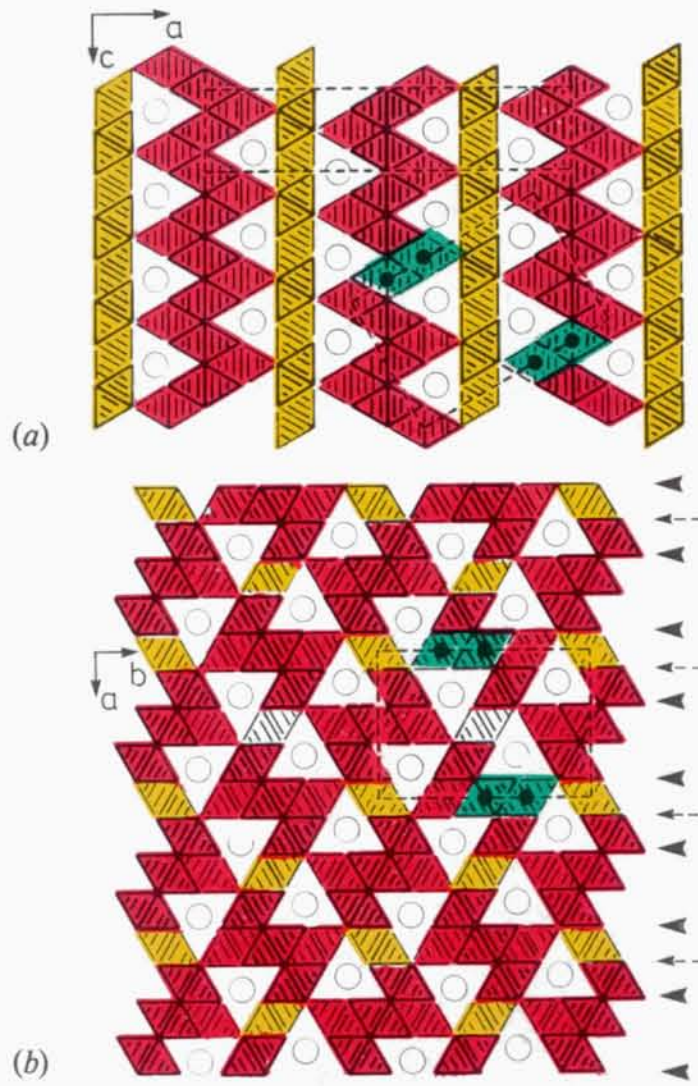

Fig. 1. (*a*) The pinakiolite structure projected along **b**. Red and yellow rhombi symbolize cation-centered octahedra at two different elevations (differentiated with thin and heavy lines). The green octahedra are those that must be rearranged to obtain the ludwigite structure. The unit cell of the (idealized) pinakiolite structure is outlined at the top of the drawing. (*b*) The structure of ludwigite projected along **c**. Compare the unit cell, with the green octahedra, with the unit shown in (*a*) found also in pinakiolite. Dotted arrows mark the plane of the slip operation that generates the structure from that of pinakiolite. The arrowheads mark the twin operation planes.

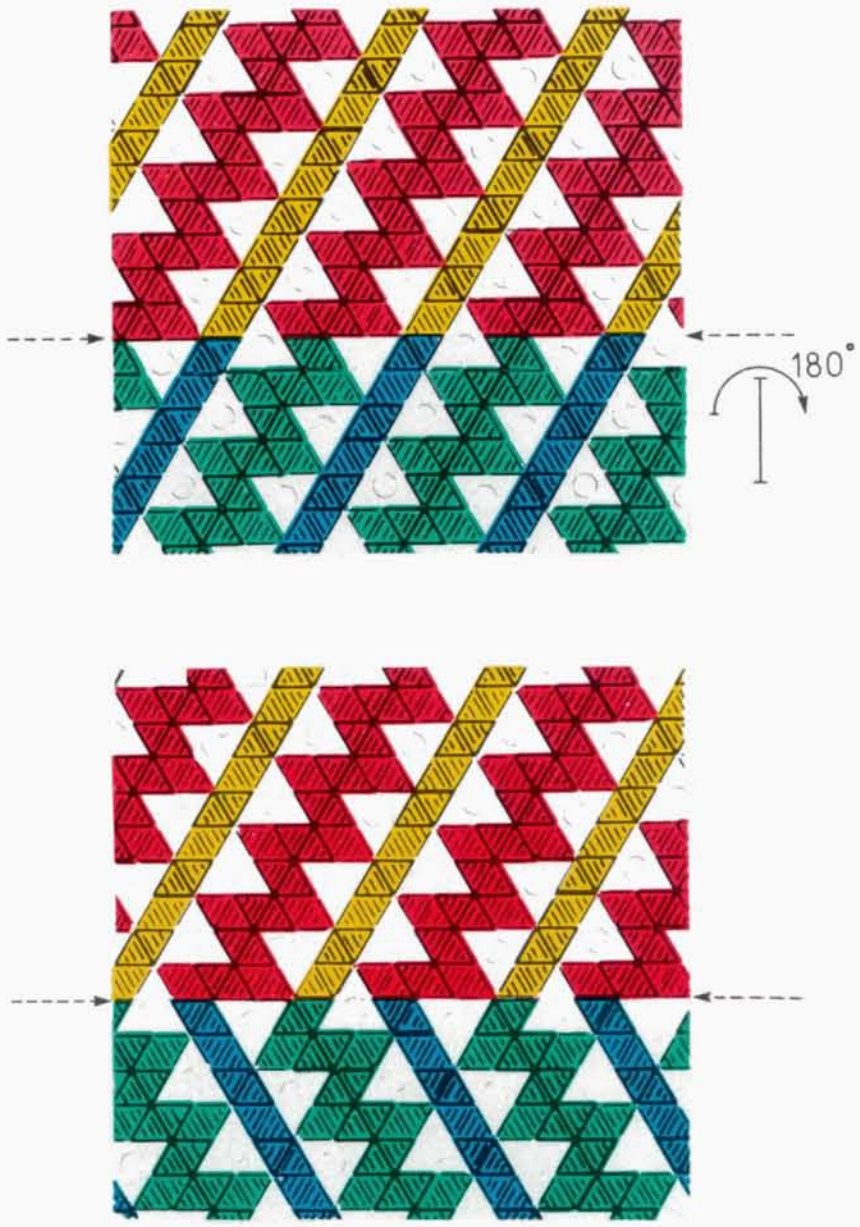

Fig. 9. Chemical twinning mechanism for the pinakiolite structure. The twin plane is marked with arrows. The twin axis and the rotation are indicated to the right of the pinakiolite structure. The final twin is illustrated below.

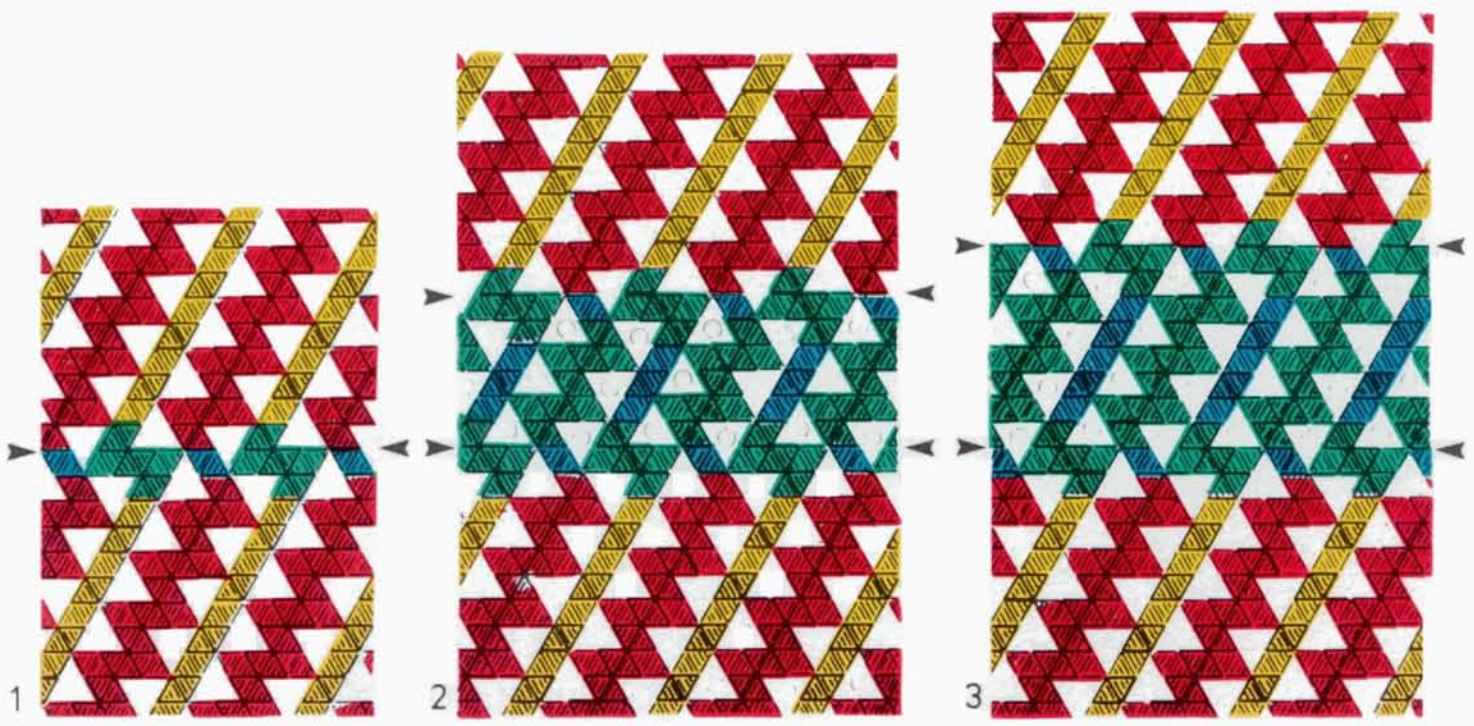

Fig. 7. Drawing of the three defects of Fig. 5. The blue and green octahedra illustrate the defect parts and include the unit cells of ludwigite (1), orthopinakiolite (2) and takéuchiite (3). The slip planes are marked with

[*To face p.* 32

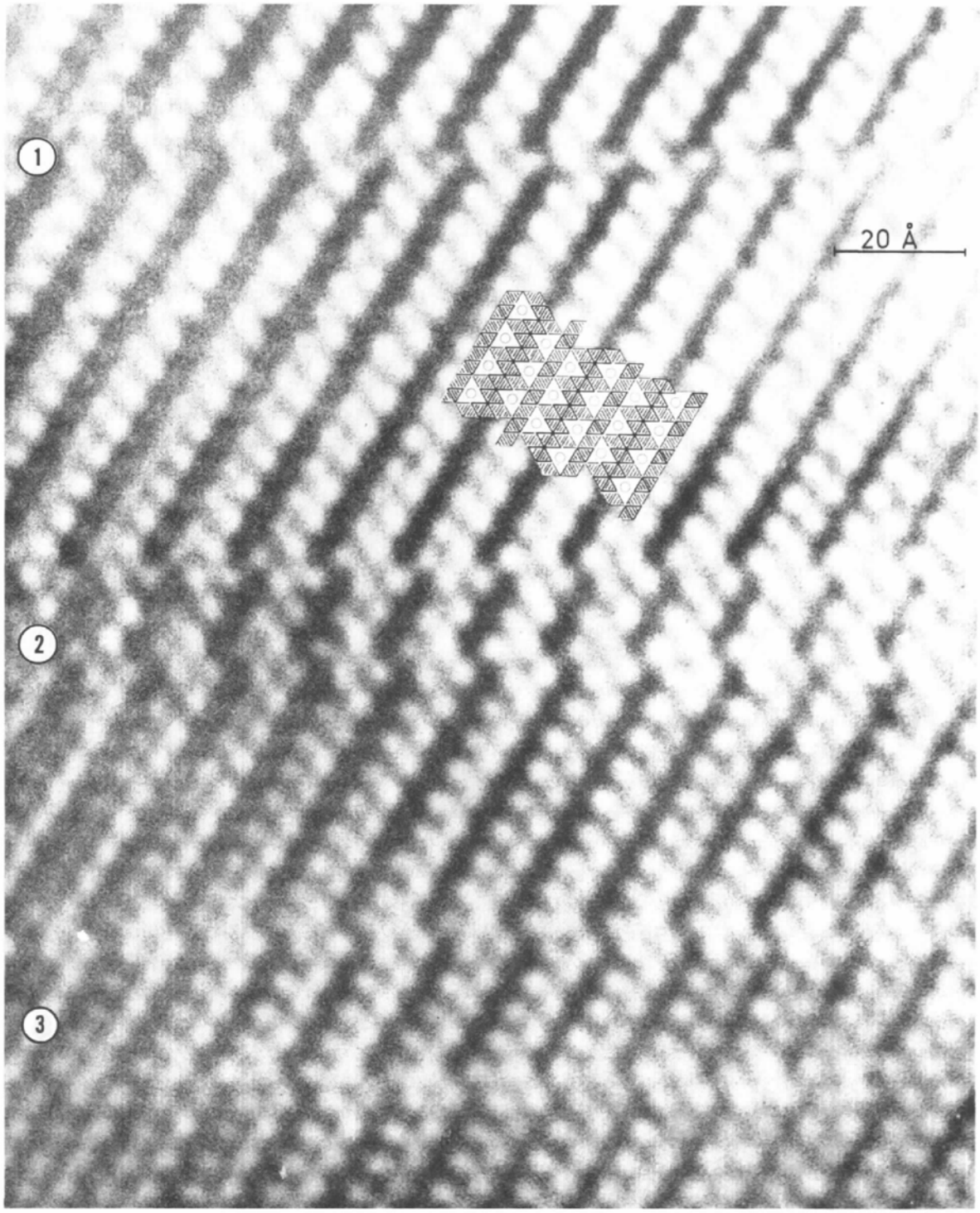

Fig. 5. Part of the electron micrograph shown in Fig. 4. The drawing is inserted for orientation and as a guide to interpretation. A possible mechanism for generation of the defect at 1 is illustrated in the drawing of Fig. 6. The structures of the defects at 1, 2 and 3 are shown in Fig. 7.

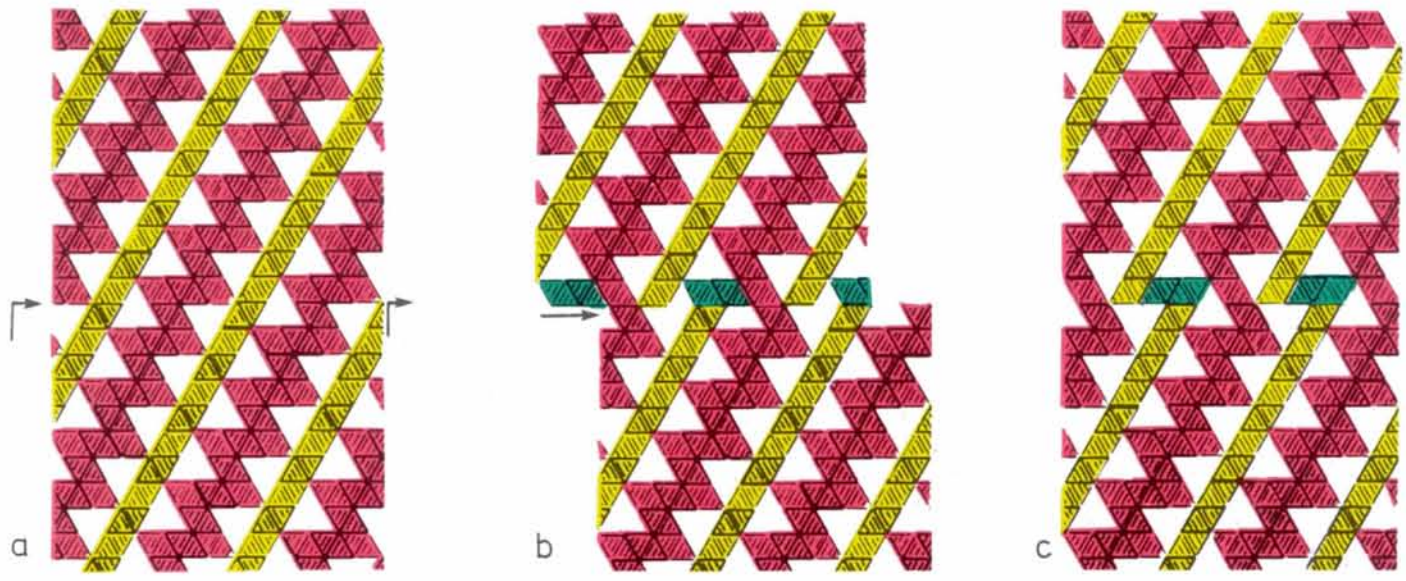

Fig. 6. Drawing illustrating a possible mechanism of generating the defect 1 in Fig. 5 from pinakiolite by the slip mechanism.

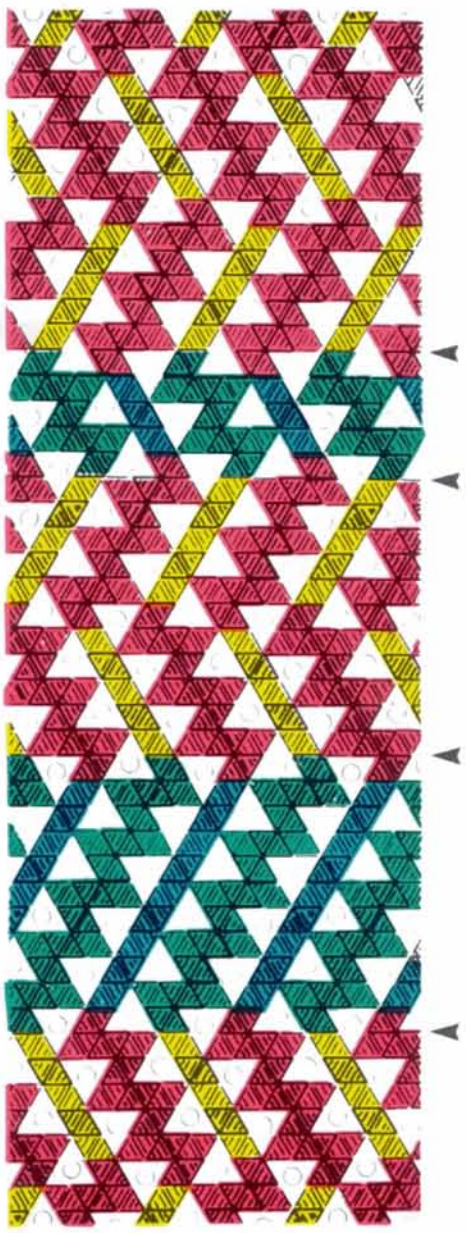

Fig. 19. Idealized drawing of the two defects shown in Fig. 18.

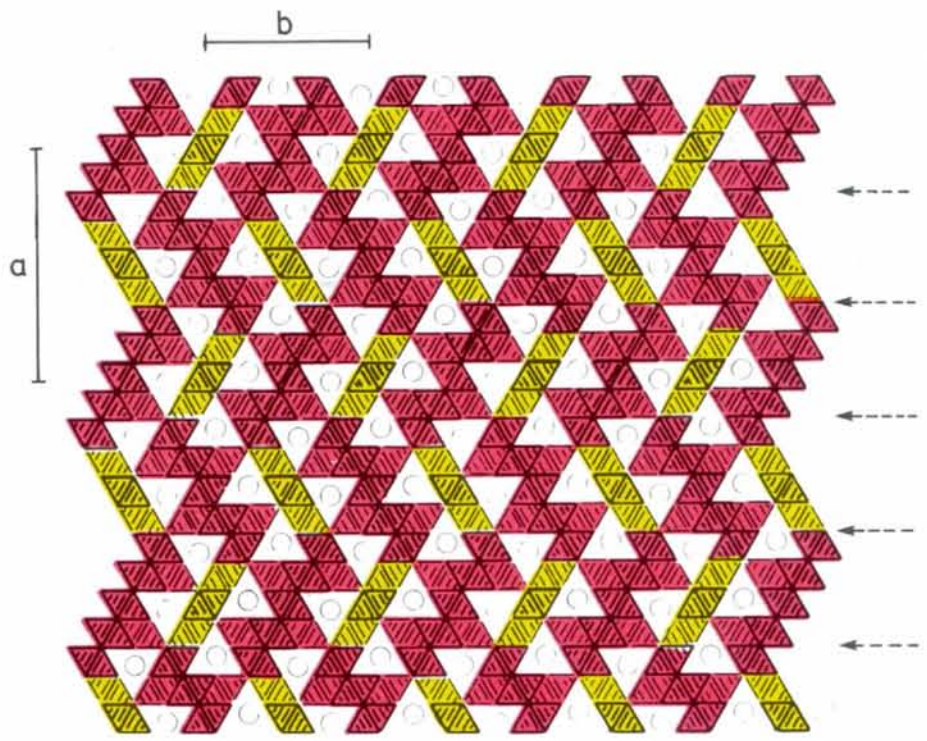

Fig. 10. Idealized drawing of the orthopinakiolite structure. Chemical twinning planes are marked with arrows.

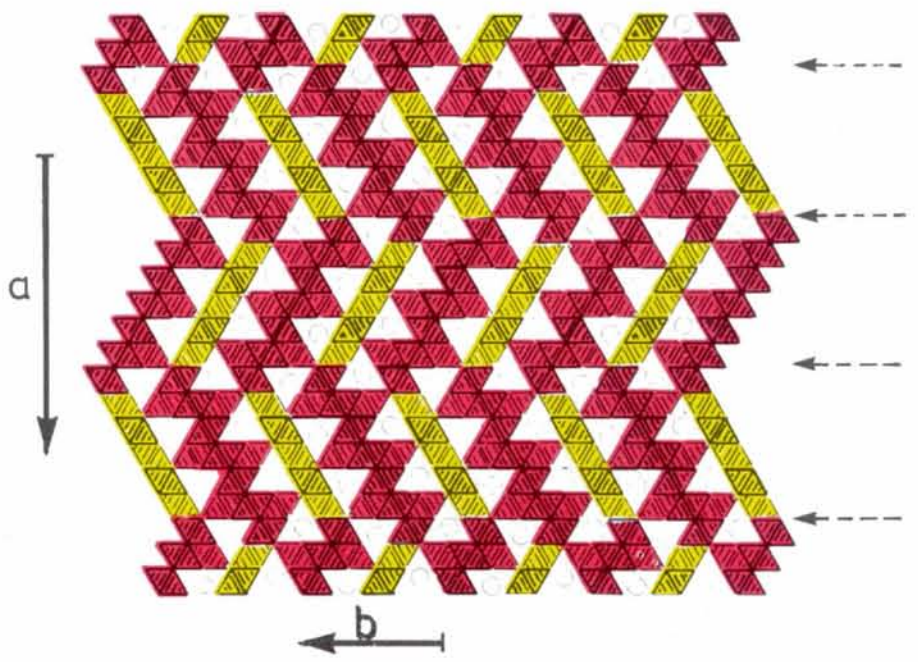

Fig. 11. Idealized drawing of the takéuchiite structure. Twin planes are marked with arrows.

walls are dark and the boron triangles are white spots as in the image of pinakiolite. The most common defects found in crystals of orthopinakiolite were, not surprisingly, caused by mistakes in the width of the twin slabs as can be seen in Fig. 15. Such broad twin slabs of pinakiolite can sometimes terminate abruptly within the crystal as in the image shown in Fig. 16. Both of the broad defects can be understood in terms of missing twin operations. The broadest one is three times *a* of the orthopinakiolite unit cell so that symbolically it can be written ...4*t*44444*t*4..., *i.e.* ...4*t*20*t*4... instead of 4*t*4*t*... in a perfect crystal. In the case of the thinner defect, the width is twice *a* and can be written ...4*t*12*t*2.... The two parts of the orthopinakiolite crystal on both sides of the broadest defect are not in phase with each other. This is obvious if the image is viewed at low angle along **a**. The same is the case for the other defect. The mismatch is the same as the distance, approximately 2·7 Å, between the centers of two octahedra in the **b** direction. Where the thin defect terminates, the structure changes from ...4*t*12*t*4... to ...4*t*4*t*4*t*4... and the surrounding structure has to adjust for the mismatch of 2·7 Å. The dark diffuse contrast in the image to the right of the termination presumably reflects this structural strain.

One crystal of orthopinakiolite showed an unusual 'crack-healing' defect as illustrated in Fig. 17(*a*). The crack is approximately 50 Å wide and the two parts of the crystal are slightly displaced as can be judged from the positions of the broad twin slabs marked with arrows in the figure. The crack must afterwards have been filled by the other material. The image of that mineral has two unit-cell axes (10·18 and 12·56 Å) in common with ludwigite (*cf.* Table 2) and the images are similar too (*cf.* Fig. 13). The selected-area electron diffraction pattern in Fig. 17(*b*) shows the intergrowth angle to be close to 30°. The orientation of the two structures does not give a favorable intergrowth boundary because it is not possible to fit the structures together without considerable distortions of the atom positions in the boundary, as indicated by the orientation of the octahedra in the origin of both structures [*cf.* Fig. 17(*a*)]. This is also indicated by the uneven phase boundary in the image.

All crystals of orthopinakiolite investigated, including those from the same specimen as Takéuchi *et al.* (1978) used for their structure determination, showed a great number of defects of the type in Fig. 15. As already remarked in the case of pinakiolite, it is likely that such defects will affect the intensity data for an X-ray structure determination and Takéuchi *et al.* (1978) also reported difficulties in refining one of the

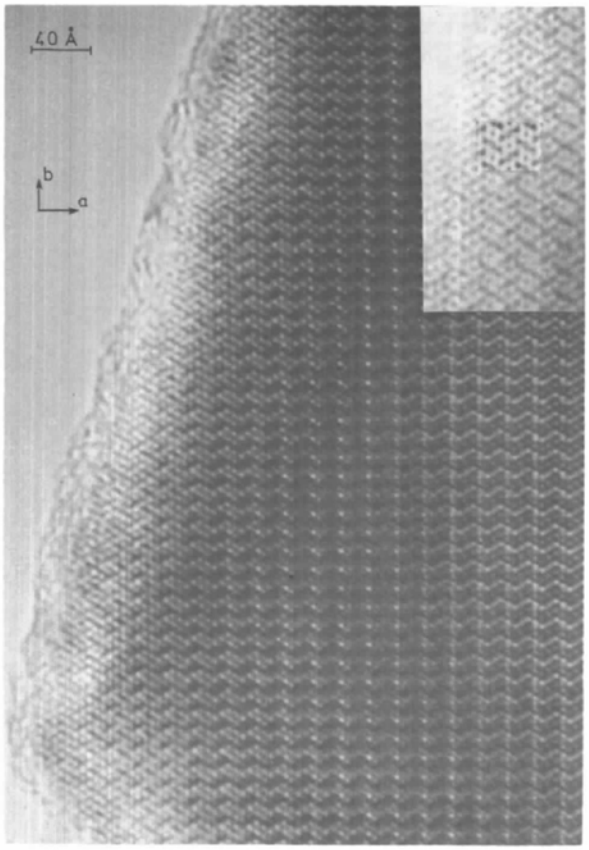

Fig. 14. Electron micrograph of an orthopinakiolite crystal recorded with the beam parallel to **c**. The image of a thin crystal is inserted at the upper right together with a calculated image (underfocus −600 Å and crystal thickness of 90 Å).

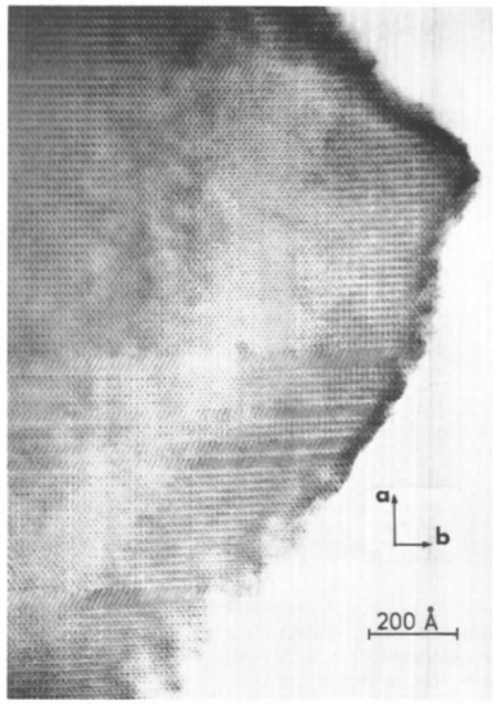

Fig. 15. An orthopinakiolite crystal showing a great number of similar defects.

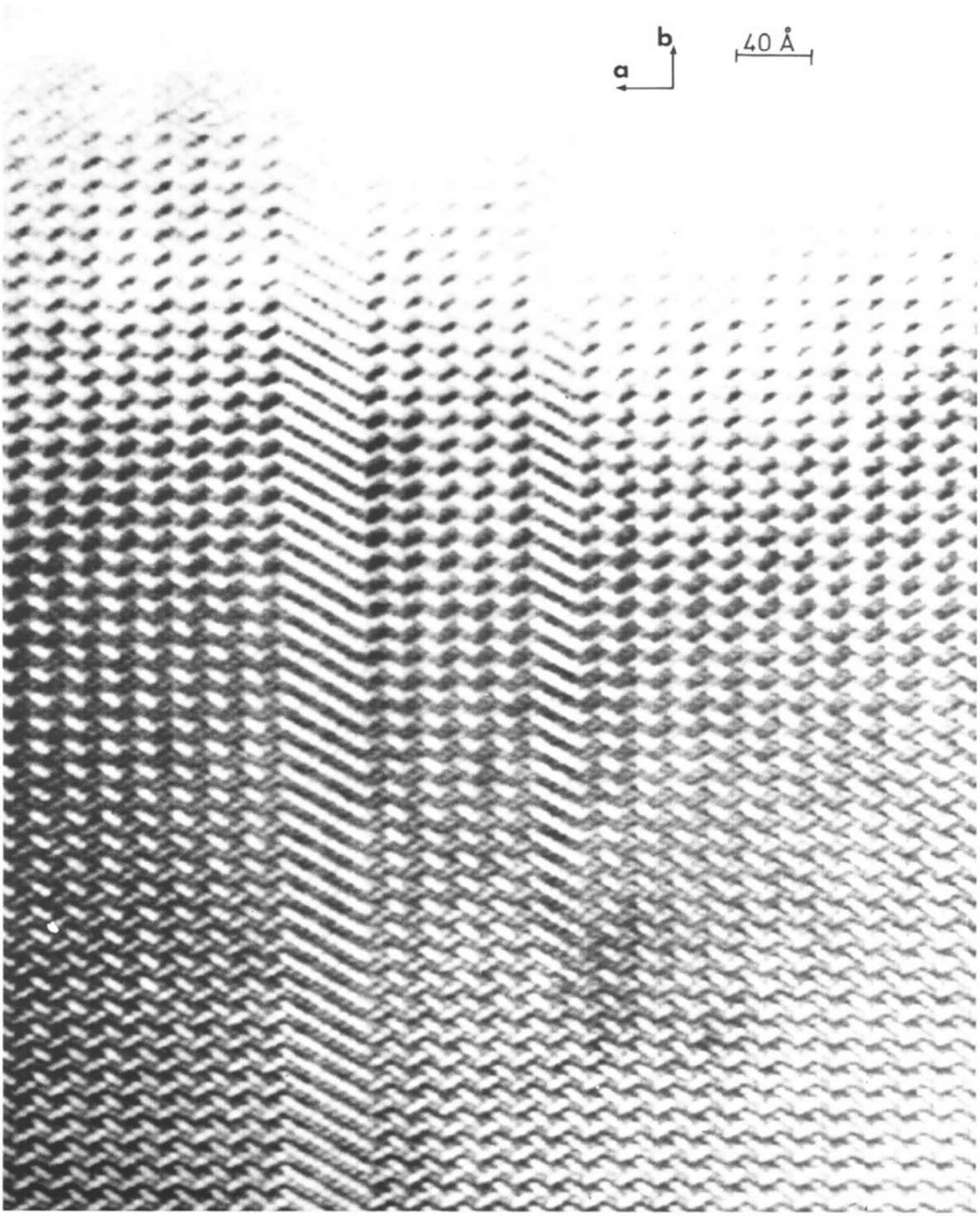

Fig. 16. Image of an orthopinakiolite crystal with a terminated defect.

cation positions. Thus position $M(7)$, which is situated in the twin plane, had to be refined as split up into three positions. The defects will probably also affect refinement of the partially unoccupied position $M(4)$.

Crystals of the new mineral takéuchiite (*cf.* Bovin & O'Keeffe, 1981) in general show fewer structural defects than orthopinakiolite crystals, although the same type of defects as found in orthopinakiolite can be found in takéuchiite crystals as is shown in Fig. 18 (*cf.* Fig. 4, Bovin, O'Keeffe & O'Keefe, 1981). The two defects marked with arrows in the figure are also illustrated in a polyhedron drawing (*cf.* Fig. 19). The two defects can be symbolized ...6*t*6*t*10*t*6*t*6*t*4*t*6*t*4.... Notice also the small crystal (65 × 40 Å) growing at the surface of the larger crystal.

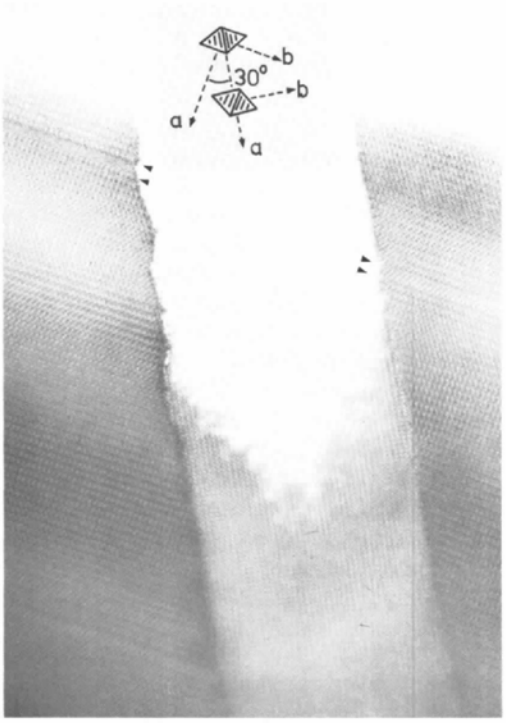

(*a*)

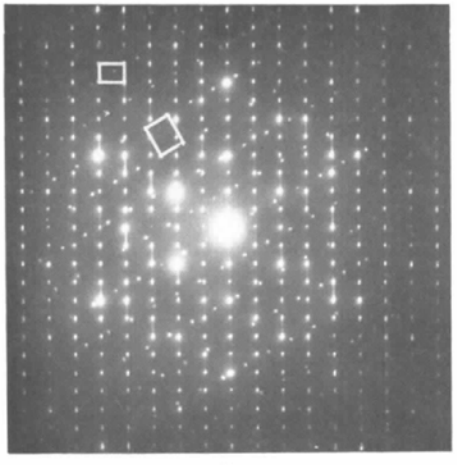

(*b*)

Fig. 17. (*a*) Electron micrograph of an orthopinakiolite crystal showing a crack joined by a ludwigite-like mineral. The corresponding defect at both sides of the crack is indicated by arrows. The orientation of the unit cells is shown in the upper part of the figure. (*b*) Electron diffraction pattern of the selected area showing a superimposed pattern of the two reciprocal cells. The small rectangle corresponds to the orthopinakiolite unit cell.

Conclusions

This investigation of the minerals of the pinakiolite family has shown that there is a close relation between the types of defect found and the structure building mechanisms of the structures. In this family it is likely that the chemical twinning mechanism plays an important role in the growth of the crystal in the **a** direction. The period of the twin operation must depend on the concentration of the different cation species in the growth environment. The frequent mistakes in the twin period can be caused by impurities or irregular fluctuations in the cation concentration.

This work has been supported by grants from the National Science Foundation (DMR 78-09197 and DMR 76-06108) and the Swedish Natural Science

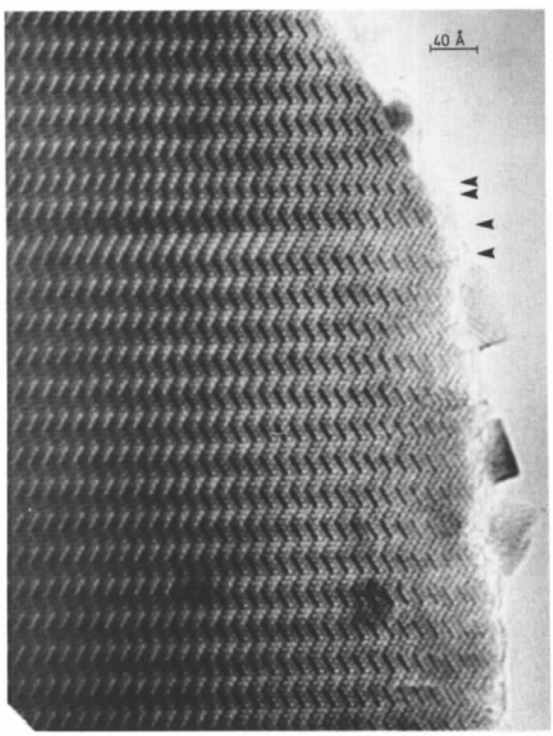

Fig. 18. Micrograph of a takéuchiite crystal showing two defects marked with arrows (*cf.* Fig. 19). The image is recorded with the electron beam parallel to **c**.

Council. We would also like to thank Mrs Ingrid Bovin and Miss Becky Vander Meade for help with coloring the drawings and Mr J. S. White Jr of the Smithsonian Institution and Dr B. Lindquist of Naturhistoriska Riksmuseet in Stockholm for making mineral specimens available for investigation.

References

ANDERSSON, S. & HYDE, B. (1974). *J. Solid State Chem.* **9**, 92–101.
BERTAUT, E. F. (1950). *Acta Cryst.* **3**, 473–474.
BOVIN, J.-O. & O'KEEFFE, M. (1980). *Am. Mineral.* In the press.
BOVIN, J.-O. & O'KEEFFE, M. (1981). *Acta Cryst.* A**37**, 35–42.
BOVIN, J.-O., O'KEEFFE, M. & O'KEEFE, M. A. (1981). *Acta Cryst.* A**37**, 42–46.
COWLEY, J. M. & MOODIE, A. F. (1957). *Acta Cryst.* **10**, 609–619.
FEJES, P. L. (1973). Thesis, Arizona State Univ.
GOODMAN, P. & MOODIE, A. F. (1974). *Acta Cryst.* A**30**, 280–290.
KONNERT, D. A., APPLEMEN, D. E., CLARK, J. R., FINGER, W. L., KATO, T. & MIURA, Y. (1976). *Am. Mineral.* **61**, 116–122.
MOORE, P. B. & ARAKI, T. (1974). *Am. Mineral.* **59**, 985–1004.
NIELSEN, K., SØTOFTE, I., THORUP, N. & NORRESTAM, R. (1978). *Acta Cryst.* A**34**, S171.
O'KEEFE, M. A. (1975). Thesis, Univ. of Melbourne.
O'KEEFE, M. A., BUSECK, P. R. & IIJIMA, S. (1978). *Nature (London)*, **274**, 322–324.
O'KEEFE, M. A. & SANDERS, J. V. (1975). *Acta Cryst.* A**31**, 307–310.
SKARNULUS, A. D. (1976). Thesis, Arizona State Univ.
TAKÉUCHI, Y. (1956). *Mineral. J.* **2**, 19–26.
TAKÉUCHI, Y. (1978). *Recent Prog. Nat. Sci. Jpn*, **3**, 153–181.
TAKÉUCHI, Y., HAGA, N., KATO, T. & MIURA, Y. (1978). *Can. Mineral.* **16**, 475–485.
TAKÉUCHI, Y., WATANABÉ, T. & ITO, T. (1950). *Acta Cryst.* **3**, 98–107.

Acta Cryst. (1981). A**37**, 35–42

Electron Microscopy of Oxyborates. II. Intergrowth and Structural Defects in Synthetic Crystals

BY JAN-OLOV BOVIN* AND M. O'KEEFFE

Chemistry Department and Center for Solid State Science, Arizona State University, Tempe, Arizona 85281, *USA*

(*Received* 19 *October* 1979; *accepted* 13 *June* 1980)

Abstract

Crystals of composition $Mg_3Mn_3B_2O_{10}$, $Mg_{3\cdot1}Mn_{2\cdot9}B_2O_{10}$ and $Mg_3(Mn_{2\cdot4}Fe_{0\cdot6})B_2O_{10}$ have been prepared at 1270 K in air and investigated by high-resolution transmission electron microscopy. Almost all crystals showed structural defects. The most common type of defect was a variation in period of chemical twinning. Slip planes and single twin planes were also found. Many crystals also showed mixed intergrowth of several structure types. Thus $Mg_3Mn_3B_2O_{10}$ crystals contained mixed intergrowth of ludwigite-, pinakiolite- and orthopinakiolite-like structures. $Mg_{3\cdot1}Mn_{2\cdot9}B_2O_{10}$ crystals contained mostly the ludwigite structure but also new long-period (82·3 Å) structures. $Mg_3(Mn_{2\cdot4}Fe_{0\cdot6})B_2O_{10}$ crystals had mainly the orthopinakiolite structure with intergrowth of ludwigite. Several new phases were identified in the electron micrographs.

Introduction

Synthetic compounds with the composition M_3BO_5, where M stands for different combinations of the ions Mg^{2+}, Mn^{2+}, Fe^{2+}, Mn^{3+} and Fe^{3+} have been reported (Bertaut, 1950; Nielsen, Søtofte, Thorup & Norrestam, 1978) to have the ludwigite structure [*cf.* Fig. 1(*b*) in the previous paper by Bovin, O'Keeffe & O'Keefe, 1981 (paper I)]. No synthetic compounds with pinakiolite, orthopinakiolite or takéuchiite structures have been reported. This investigation of synthetic members of the pinakiolite family was undertaken in order to reveal the 'true' structure of crystals prepared with different cation concentrations. From the structural

* Permanent address: Inorganic Chemistry 2, Chemical Centre, PO Box 740, S-220 07, Lund 7, Sweden.

0567-7394/81/010035-10$01.00